https://dx.doi.org/10.1016/j.energy.2022.125426

Revisiting the pricing benchmarks for Asian LNG — An equilibrium analysis

Lingge Zhang[1], Dong Yang*[1], Shining Wu[1], Meifeng Luo[1]

[1] Department of Logistics and Maritime Studies, The Hong Kong Polytechnic University

* Corresponding author, Email: dong.yang@polyu.edu.hk

Abstract

As the spot natural gas price in Asia decoupled from the oil price, increasing researchers argued that the oil-indexed pricing mechanism cannot reflect the market fundamentals of Asian liquefied natural gas (LNG). This study investigates if the Japan-Korea-Marker (JKM) price is a feasible pricing benchmark to replace the oil price. For this purpose, we propose an equilibrium pricing model for the LNG long-term contract (LTC) in Asia. Our model incorporates the risk-averse importer and exporter who optimize their risk-profit tradeoffs by deciding their LTC-spot trade portfolios. Using the model, we compare the pricing efficiency and the risk-profit tradeoff of an importer/exporter under different benchmarks (oil price versus JKM price). The results show that the JKM price is more efficient as an LTC pricing benchmark than the oil price. The JKM pricing benchmark is favored for both exporters and importers when they are low risk-aversion. In addition, we compare the performance of the JKM benchmark based on the CIF price term (i.e., the importer pays for freight charges) with that based on the FOB price term (i.e., the exporter pays for freight charges). We find that the freight liability has little effect on the pricing efficiency of the JKM benchmark.

Keywords: LNG pricing, Oil indexation, Japan-Korea-Marker, Equilibrium, Long-term contract, Risk sharing

1. Introduction

The global natural gas market is regarded as a composite of three relatively independent regional markets (North America, Europe, and Asia), each with significant price differentials. In the Asian market, the gas price over the last ten years has generally been higher than that in Europe and North America, a phenomenon often called the "Asian premium" (as shown in Figure 1).

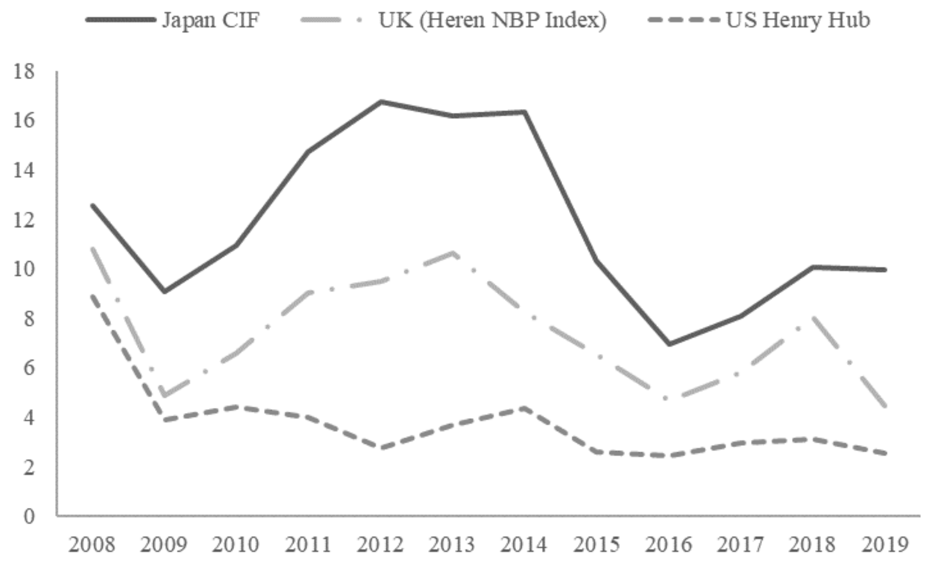

Figure 1. Natural gas prices in Asia, Europe and North America from 2008 to 2019 (unit: US$/MMBtu). *Source*: *British Petroleum (BP) Company, 2020.*

The high price of LNG in the Asian market has once been attributed to the market fundamentals of Asian natural gas, namely, supply, demand, and transportation cost (Neumann and Hirschhausen, 2015). As Vivoda (2014) explained, the major gas-consuming countries in Asia are highly dependent on liquified natural gas (LNG) imports from distant gas sources. In 2019, Asia was the largest gas-importing region: it accounted for 39.3% of the global gas trade, of which 86.26% was in the form of LNG (BP, 2020). The high importing demand with the expensive transportation cost (freight rate of LNG is traditionally higher than transmission fee of the pipeline) eventually results in high gas prices.

However, recent studies have found that the oil pricing mechanism that dominates in the Asian LNG trade, rather than the market fundamentals, is the determinant of high LNG prices in Asia (Zhang et al., 2018a; Shi and Shen, 2021; Li et al., 2020). Therefore, doubts about the rationality of the oil-indexed pricing mechanism are growing in the Asian LNG market. Essentially, the oil-indexed pricing mechanism is founded on the assumption that the oil and natural gas are substitute fuels. Some argue these two fuels are not perfect substitutes and have different driving factors of market fundamentals (Zhang et al., 2018b). It implies that the oil-indexed pricing mechanism is inefficient to reflect the supply and demand of the Asian LNG market. Stern (2014) noted that some exogenous shocks, e.g., the shale gas revolution, Fukushima nuclear accident, had a profound impact on the gas supply and demand, while this impact was not reflected in the oil-indexed gas price. In practice, price decoupling between the oil price and the LNG spot price in the Asian LNG market makes it more conceivable that the oil-indexed pricing mechanism is inefficient (Zhang and Ji, 2018). In particular, the COVID-19 crisis exacerbated gas oversupply by dampening gas demand. This led to the record-low LNG spot price, which intensified Asian LNG price decoupling (Ason, 2020). This phenomenon suggests that LNG market fundamentals are less correlated with oil prices and thus that oil-indexed pricing has become untenable (Stern and Imsirovic, 2020).

Given this, creating an Asian LNG spot trading hub has been proposed as a solution for efficiently pricing LNG (Shi and Variam, 2017). As other gas trading hubs (e.g., the Henry hub for the United States) determine the price of natural gas based on gas-to-gas competition within a market, it is possible that the hub price can be an efficient benchmark for reflecting LNG demand and supply in pricing long-term contracts (LTCs), futures, and other derivatives (Zhang et al., 2018a). As there currently exists no LNG trading hubs in Asia, it is more practical for Asian gas importers to find an existing benchmark to improve the pricing efficiency. Recently, the Japan-Korea Marker (JKM) price published by Platts is gaining attraction, with the rapid expansion of the LNG spot trade in Asia (Stern and Imsirovic, 2020).

This paper, therefore, aims to investigate whether using the JKM price as the pricing benchmark is a feasible solution to improve the LNG pricing efficiency in Asia. In order to answer this question, two basic conditions need to be evaluated. First, we must ascertain whether the JKM price performs better than the oil price in reflecting LNG supply and demand in Asia. Second, we must determine whether both gas importers and exporters are willing to accept the new benchmark. Furthermore, we have to address the concerns of industry veterans regarding the low transparency of the JKM benchmark (due to its daily, inquiry-based price formation). The inquiry only provides a final price to gas importers, and the opacity of the trade cost thus leaves exporters room for hidden margins (Palti-Guzman, 2018). In comparison to the current JKM cost-insurance-and-freight (CIF) price, the free-on-board (FOB) price transfers the transportation costs from exporters to importers, thereby increasing transparency. Inspired by this, we will also explore whether the JKM FOB performs better than the JKM CIF as an LNG pricing benchmark.

Some empirical studies have illustrated that the JKM price is more efficient than the oil price in serving as a benchmark for LNG pricing (e.g., Alim et al., 2018). These studies, however, fail to evaluate the reactions of importers and exporters, as empirical methods are unable to look into the black box of market mechanisms. In order to fill this gap, we build an equilibrium model for LTC pricing in the Asian LNG market. This model is built upon a mean-variance expected utility framework. This framework is commonly used in equilibrium analysis of the electric power market (Bessembinder and Lemmon, 2002; Gersema and Wozabal, 2017). In order to apply it in the LNG market, we modify the model by considering following two characteristics of the Asian LNG market. First, natural gas is a storable commodity, while electricity is not. For electricity, it is impossible to buy a certain amount of electricity in one period and then hold it for the next-period sale. In our model, therefore, we add a non-negative inventory constraint so as to retain the possibility that the importer conducts intertemporal arbitrage in the LNG spot market. Second, based on the fact that Asian LNG trades at the CIF price, our model considers freight fluctuations. This modification allows us to explore the feasibility of using the JKM FOB benchmark, via analysis of the impact of freight rate transfers between importers and exporters on natural gas pricing.

Based on the proposed equilibrium model, we can investigate and compare the pricing efficiency of possible benchmarks (i.e., oil prices, the JKM CIF price, and the JKM FOB price) via the LTC's risk sharing function. The risk sharing of an LTC is reflected in its take-or-pay (TOP) clause. This clause stipulates that the importer bears the LNG volume risk and the exporter takes the price risk (Abada et al., 2017). This risk sharing by means of the TOP clause is effective, if the pricing benchmark of an LTC is efficient in reflecting the supply and demand for natural gas within a market. Additionally, the model allows us to estimate the risk-profit tradeoff of importers and exporters, based on their LTC-spot trade portfolio. By comparing the risk-profit tradeoff under different benchmarks, we can directly judge the benchmark that a given importer or exporter would be likely to accept.

Based on historical data, we forecast the future dynamics of candidate benchmarks which are input into the model. The results of numerical study show that the JKM CIF/FOB price is more efficient than the oil price as a pricing benchmark of LNG LTC. This is due to the fact that the JKM pricing benchmark can help importers to create more effective hedging positions in their LTCs. This benchmark is favored for exporters and importers if both of them are low risk-averse. In addition, the JKM pricing benchmark can effectively prevent the transfer of price risk from an LNG exporter to the importer in the high-risk-aversion case.

The rest of this paper is organized as follows: Section 2 reviews the existing literature on the topic, and summarizes the contributions of this study. Section 3 describes the equilibrium pricing model constructed for the Asian LNG market. Section 4 simulates the random inputs of the equilibrium model based on real data. Section 5 compares the model results of different pricing benchmarks. Section 6 presents the conclusions of this paper.

2. Literature review

With the growth of spot trading and gas-oil price decoupling in Asia, the so-called "Asian premium" is attracting attention from studies on Asian LNG prices. Recently, researchers have explored the origins of this phenomenon. Zhang et al. (2018a) compared the price determinants of gas markets in the US, Germany, and Japan. Shi and Shen (2021) followed Zhang et al. (2018a), and put their focus on the macroeconomic uncertainties surrounding the gas market. Using a vector autoregressive (VAR) model, these two studies indicated that the oil-indexed pricing mechanism was accountable for the "Asian premium." Another group of literature on the origins of the "Asian premium" investigated price bubbles within regional natural gas markets. Zhang et al. (2018b) adopted a generalized sup augmented Dickey-Fuller test to explore gas price bubbles in the US, Europe, and Japan. Taking the same approach, Li et al. (2020) further identified the periodicity of gas price bubbles in these three markets. Both studies concluded that the price differential in the Asian LNG market was a spillover effect from the oil market. The aforementioned studies also proposed policies to address the pricing inefficiency, such as building an LNG trading hub (Zhang et al., 2018a; 2018b), and using the JKM price as the pricing benchmark (Alim et al., 2018). The effectiveness and feasibility of these policies, however, have not yet been evaluated.

An evaluation of these policies directed toward the Asian premium is an investigation of whether to retain the oil-indexed pricing mechanism for the natural gas trade. Numerous studies have provided empirical evidence on this point by exploring the relationship between the gas spot price and the oil price. Early studies focused on cointegration analysis of these two prices. Brown and Yücel (2008), and Hartley et al., (2008) concluded that the oil-indexed gas price was reliable, as they found the long-term equilibrium between the two prices. Doubts about the reliability of this conclusion emerged, however, with the finding that the cointegration of these prices was volatile over time (Erdős, 2012; Ramberg and Parsons, 2012). In order to capture the time-varying characteristics of prices, Brigida (2014) and Asche et al. (2017) applied regime-switching models to investigate the US and UK gas markets, respectively. Both of them verified that price cointegration existed, but with instability. Geng et al. (2016) applied the same approach in order to explore the impact of the shale gas revolution on natural gas prices. They found that the shale gas revolution intensified the gas-oil price decoupling within the US market.

With the advent of novel empirical approaches and the availability of sophisticated databases, some literature began to incorporate more of the complexities related to the dynamic and nonlinear features of the gas-oil nexus. Batten et al. (2017) employed time- and frequency-domain causality tests so as to analyze the time-varying spillover effect between the gas spot price and the oil price. They concluded that the two prices in the US have been almost independent after the 2008 financial crisis. Zhang and Ji (2018) applied a long-memory approach, and showed strong evidence of price decoupling in the US; meanwhile, the gas-oil price nexus still held in Europe and Asia. Wang et al. (2019) applied a dynamic model averaging (DMA) approach in order to explore the driving factors of gas prices in the US market. The results suggested that the effect of supply and demand was more significant than that of the oil price on the gas spot price. Lovcha and Perez-Laborda (2020) also analyzed the oil-gas price volatility spillover via the framework of dynamic frequency connectedness. They found that the magnitude of the spillover effect varied over time, but that the volatilities of the two prices were not decoupled. Ftiti et al. (2020) examined the dynamic gas-oil relationship via both linear and nonlinear machine learning models. They found that the gas-oil relationship more closely resembled a nonlinear one, which depended on the existence of extreme price movements in the tested time scales. It is clear that these empirical studies did not arrive at a consensus on the gas-oil price relationship, due to the differences in methodologies, markets analyzed, and data sample periods. More importantly, these studies cannot explicitly showcase the impact of either retaining or abandoning this pricing mechanism on participants in the natural gas trade.

The equilibrium model proposed in this study is built upon the decision-making of market participants, which allows us to excavate the mechanism that underlies the effects of the proposed policies. There are many deterministic and stochastic equilibrium models for natural gas market (e.g., Zhuang and Gabriel, 2008; Egging et al., 2010; Guo and Hawkes, 2018). These models have been successfully applied to evaluate the implications of various policies, including market entrance (Feijoo et al., 2016), energy structure transition (Holz et al., 2016), and pricing schemes (Shi and Variam, 2017). For instance, Egging et al. (2017) proposed an equilibrium model that considered risk-averse agents within the European gas market. This model was applied to analyze the effects of uncertain shale gas exploration on the investment choices of gas suppliers. The results suggested that the high risk-averse disposition of suppliers leads to lower investment, thereby causing gas prices to rise. Abada et al. (2017) presented an equilibrium model that endogenized the long-term contract behavior of risk-averse gas producers and midstreamers. This study is a typical example of using an equilibrium model to analyze the gas pricing mechanism. Using the model, they showed that the oil-indexed LTC is still attractive in the European gas market, as it provides financial security for European producers (who bear expensive investment costs). There exist few studies, however, that apply the equilibrium model to studying risk management and risk aversion (which also affect the gas trade), and none of the existing studies focus on the Asian market.

The contribution of this paper is thus threefold. First, through building an equilibrium pricing model that accounts for risk aversion, we provide a new perspective for analyzing the pricing mechanism in the Asian LNG market. We examine not only the efficiency of different pricing benchmarks, but also their effects on the risk-profit tradeoff calculations of market participants. This is a crucial consideration for implementing a pricing mechanism. Second, we enrich the equilibrium model and its incorporation of risk aversion by considering the particular characteristics of the LNG market. We compare the FOB-based pricing with CIF-based pricing in order to explore the effects of freight rate transfers on improving the performance of pricing benchmarks. Third, we find that using the JKM price as the pricing benchmark can improve the pricing efficiency for LTCs. This finding has important practical significance for the selection of pricing benchmarks in the Asian LNG market.

3. Model

In this section, we construct an LTC equilibrium pricing model. In particular, Section 3.1 provides the assumptions and nomenclature of the model. We define the agent's profits in Section 3.2. In Section 3.3, we display the optimization problems for both exporters and importers, and the market clearing conditions.

3.1 Model assumptions and nomenclature

In this study, we assume that all participants in the LNG trade are homogenous, and that they can be represented by two representative agents, namely exporter and importer. We focus on a bilateral transaction between an exporter and an importer. The exporter sells LNG to the importer, either via LTC or spot market. The importer purchases LNG so as to meet the consumption within a market, or to resell it in a spot market. The importer cannot directly resell the gas in LTC, due to the restriction of destination clause (Shi and Variam, 2016). Competition within the market is assumed to be perfect, which implies that the importer and the exporter alike are both price takers. In addition, we assume that both the exporter and the importer have the same expectations of prices, as the market information (e.g., futures prices of oil and LNG) is consistent for each of them.

In general, a standard LTC of LNG has a 20-year contract period, which is too long a period for us to make a persuasive forecast of LNG market trends. Alternatively, we divide the whole LTC period into several trading periods (e.g., one year) and focus our study on one of those periods. The rationality of this setting is supported by examples of LTC price renegotiation in reality, for example, the renegotiation between India and Australia in 2017. Through the renegotiation, Australia reduced the LTC price for India from 14.5% of the Japanese crude import price to 13.9% of the Brent oil price[1]. Due to the change in the LTC price, the contract before and after the renegotiation can be regarded as separated trading periods.

As an example, Figure 2 showcases the dynamics of the first trading period after entering into an LTC. At initial time 0, an LTC for LNG is concluded between the exporter and importer. In addition to total trade volume and the pricing benchmark throughout the whole contracting period, the LTC specifies the delivery volume in each trading period, and the base price in the first trading period. In the trading period between time 0 and T, the LNG is delivered in batches at specified delivery times $(1, 2, \ldots, T)$. The interval of two adjacent times constitutes one delivery period of LNG. For example, the interval between time 0 and time 1 is the first delivery period, marking the commencement of the contract. At each delivery time t, the corresponding batch of LTC delivery is completed, and the spot trade of both the exporter and the importer finishes clearing. For the purpose of simplification, we assume that the delivery volume of LTC is equal at every delivery time. At the ending time T, with the completion of the last batch of LTC delivery, the contract settlement for the first trading period is finished. After finishing the first-period trade of LTC, the contract parties will review the contract in order to determine the base price for the next trading period. The contract will continue by following the above process, but with a new base price. Each trading period is also accompanied by market uncertainty, we assume that the market uncertainty only comes from the volatility of the LNG spot price, the price benchmark, and spot freight rates.

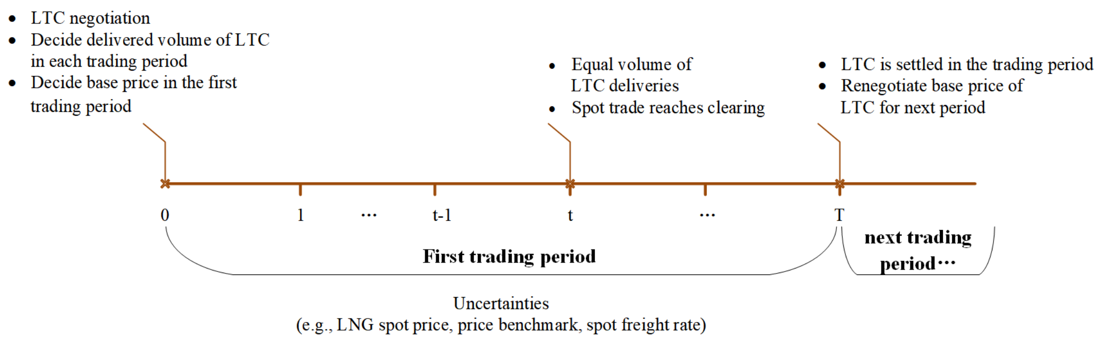

Figure 2. Dynamics of a trading period under an LNG long-term contract

[1] Detailed information was reported by LiveMint in 2017, and available at https://www.livemint.com/Money/MpJAxVSQwMExq5KmfpYGJL/The-gains-from-the-Gorgon-LNG-contract-renegotiation.html

We define the mathematical notations of the model, as follows:

Indices	
h	Superscript denoting agent, $h \in H = \{s, b\}$, where s denotes the LNG exporter, and b denotes the LNG importer.
t	Subscript denoting the discrete time in a trading period (e.g., one year), $t \in \{0, \dots, T\}$. When $t = 0$, it indicates the initial time of the trading period. When $t \in \{1, \dots, T\}$, it indicates a delivery time within the trading period.
LTC	Superscript denoting Long-term contract (for both LNG trade and shipping).
SPM	Superscript denoting spot market (for both LNG trade and shipping).
OIL	Superscript denoting oil market.
CPM	Superscript denoting gas consumption market.
Variables	
q	Trade volume of LNG
p	Price of LNG or oil
f	Freight rate of LNG
π	Profit of agent
w	Revenue of agent
ϕ	Cost of agent
Parameters	
γ^h	Attitude of the agent towards risks, if $\gamma^h = 0$, the agent is risk neutral; if $\gamma^h > 0$, the agent is risk averse.
κ	Binary parameter indicating whether exporter or importer pays for freight rate.
δ	Binary parameter indicating the pricing benchmark.
d	LNG consumption demand.
Q	LNG production/regasification capacity of agent.

In this study, we clarify that a tilde on a variable $\tilde{x}$ indicates that the variable is random, while a bar on a variable $\bar{x}$ indicates that the variable is exogenous, and acting as a parameter. Additionally, variables in the model are nonnegative unless otherwise stated.

3.2 Definition of agent profits

For an exporter, its total profit is obtained from LNG sales, via both spot market and LTC.

$$\tilde{\pi}^s = \tilde{\pi}^{s,SPM} + \tilde{\pi}^{s,LTC}, \tag{1}$$

where $\tilde{\pi}^s$ is the total profit of the exporter, and $\tilde{\pi}^{s,SPM}$ and $\tilde{\pi}^{s,LTC}$ are the profits from LTCs and spot trades, respectively. The spot profit of an exporter is defined as follows:

$$\tilde{\pi}^{s,SPM} = \sum_{t=1}^{T} \left(\tilde{p}_t^{SPM} - \tilde{f}_t^{SPM}\right) q_t^{s,SPM}, \tag{2}$$

where $\tilde{p}_t^{SPM}$ and $\tilde{f}_t^{SPM}$ are the spot CIF price of LNG, and the spot freight rate at delivery time t, respectively; $q_t^{s,SPM}$ indicates the LNG spot sales at t. We only consider the freight rate in formulating the exporter's profit. The reason for this is that the trading period set in this model is a relatively short term (one year). Other costs (namely, production costs) in that period can be regarded as constant, and thus have no effect on the market risks that the exporter takes.

The key to defining the LTC profit of an exporter is the LTC pricing function. We formulate the LTC price as the sum of the base price and the variation of the pricing benchmark, which is shown in following equation:

$$\begin{aligned}\tilde{p}^{LTC} = p_0^{LTC} &+ \delta(\tilde{p}_T^{OIL} - \bar{p}_0^{OIL}) \\ &+ (1-\delta)\left[\left(\tilde{p}_T^{SPM} - \kappa \tilde{f}_T^{SPM}\right) - \left(\bar{p}_0^{SPM} - \kappa \bar{f}_0^{SPM}\right)\right],\end{aligned} \tag{3}$$

where $\tilde{p}^{LTC}$ is the settlement price of the LTC, $\bar{p}_0^{OIL}$ is the LTC base price negotiated at time 0, $\bar{p}_0^{OIL}$ and $\tilde{p}_T^{OIL}$ denote the oil price at initial time 0 and ending time T, respectively. All prices at the beginning of the trading period ($t = 0$) can be observed by both the importer and the exporter, thereby rendering them exogenous. As our assumption on LTC execution only allows the LTC to be settled at the end of the trading period ($t = T$), the benchmark variation is the price difference between time 0 and time T. When the binary parameter δ equals 1, the LTC is benchmarked according to the oil price. Otherwise, it is benchmarked by the LNG spot price. For the case of the LNG spot pricing benchmark, we further split our price analysis into CIF-indexed and FOB-indexed benchmarks via binary parameter κ. When κ equals 0, the LNG spot pricing benchmark is the CIF. Otherwise, it is an FOB-based benchmark.

We describe the LTC profit of a given exporter as follows:

$$\tilde{\pi}^{s,LTC} = \left(\tilde{p}^{LTC} - \kappa \bar{f}^{LTC}\right) q^{s,LTC}, \tag{4}$$

where $q^{s,LTC}$ denotes the LNG volume that the exporter sells through the LTC during the trading period. We assume that the LTC binds a long-term chartering contract (LCC) with LNG tankers. Our rationale is that the long-term chartering contract can provide a stable fleet capacity so as to ensure that the LTC volume can be delivered during a given trading period. In order to simplify it, we assume the long-term freight rate $\bar{f}^{LTC}$ is fixed. The parameter κ in equation (4) is consistent with that in equation (3). The implication of this is that, if the pricing benchmark is CIF/FOB, $\tilde{p}^{LTC}$ is a CIF/FOB price. It should be noted that $\tilde{p}^{LTC}$ is a CIF price ($\kappa = 1$) when the oil-indexed benchmark ($\delta = 1$) is adopted.

An importer purchases LNG from the exporter, both through LTCs and spot market trades. A given importer's purchasing cost is described as equation (5):

$$\tilde{\phi}^b = \left[\tilde{p}^{LTC} + (1-\kappa)\bar{f}^{LTC}\right]q^{b,LTC} + \sum_{t=1}^{T} \tilde{p}_t^{SPM} q_t^{b,SPM+}, \tag{5}$$

where $\tilde{\phi}^b$ is the total purchasing cost of the importer within the trading period, $q^{b,LTC}$ is the LNG volume that the importer purchases via LTC, and $q_t^{b,SPM+}$ denotes the spot LNG volume that the importer purchases at delivery time t. $(1-\kappa)$ in equation (5) ensures that the type of $\tilde{p}^{LTC}$ (CIF or FOB) is consistent with that in equation (4). The importer can either sell the purchased LNG in the gas consumption market, or resell it in a spot market. The revenue that the importer obtains can be described as follows:

$$\widetilde{w}^b = \bar{p}^{CPM}\left(q^{b,LTC} + \sum_{t=1}^{T} q_t^{b,SPM+} - \sum_{t=1}^{T} q_t^{b,SPM-}\right) + \sum_{t=1}^{T} \tilde{p}_t^{SPM} q_t^{b,SPM-}, \tag{6}$$

where $\widetilde{w}^b$ is the total revenue of the importer, and $\bar{p}^{CPM}$ indicates the gas price in the consumption market. We assume that this price is fixed during the trading period. $q_t^{b,SPM-}$ is the LNG volume that the importer resells in a spot market. According to equations (5) and (6), we can define the importer's profit as:

$$\tilde{\pi}^b = \widetilde{w}^b - \tilde{\phi}^b - \sum_{t=1}^{T} \tilde{f}_t^{SPM} q_t^{b,SPM-}, \tag{7}$$

where $\tilde{\pi}^b$ is the total profit of the importer, $\tilde{\pi}^b$ is not solely the revenue after subtracting the purchasing cost: as the spot market in Asia is still dominated by bilateral physical trade, transportation costs are inevitable (Abada et al., 2017). Therefore, freight charges for reselling LNG (i.e., the last portion of equation (7)) also need to be deducted in order to determine total profit.

3.3 Market equilibrium model

As we mentioned in Section 1, our model is based on the mean-variance expected utility framework. The expected utility function is displayed as follows:

$$\mathbb{E}[U(\tilde{\pi}^h)] = \mathbb{E}(\tilde{\pi}^h) - \frac{\gamma^h}{2} Var(\tilde{\pi}^h), \ \ \forall h \in H = \{s, b\}, \tag{8}$$

The expected utility $\mathbb{E}[U(\tilde{\pi}^h)]$ of an agent h is linearly correlated with its expected profit, and the profit-related risk is measured by the variance of profit. γ^h denotes the willingness of each agent to accept risks. In this study, we assume that both the importer and the exporter are risk-averse, so γ^h is a positive parameter. Through utility maximization, each of the two agents can achieve a balance between their profits and the corresponding risks. The equilibrium model, therefore, is assembled by integrating the utility maximization problems of each agent, together with the market clearing conditions in both LTC and spot trade transactions.

The utility maximization of the importer is shown as:

$$\max_{q^{b,LTC},q_t^{b,SPM+},q_t^{b,SPM-}} \mathbb{E}[U(\tilde{\pi}^b)] \tag{9}$$

Subject to

$$\frac{q^{b,LTC}}{ord(T)} + q_t^{b,SPM+} \leq Q^b \quad (\lambda_t^b),\ \ \forall t \in \{1,2,\dots,T\}, \tag{9.a}$$

$$\begin{aligned}\frac{q^{b,LTC}}{ord(T)} + q_t^{b,SPM+} - q_t^{b,SPM-} + (ord(t)-1)\frac{q^{b,LTC}}{ord(T)} \\ + \sum_{t'<t}\left(q_{t'}^{b,SPM+} - q_{t'}^{b,SPM-} - d_{t'}\right) - d_t \\ \geq 0 \quad (\mu_t^b),\ \ \forall t,t' \in \{1,2,\dots,T-1\},\end{aligned} \tag{9.b}$$

$$q^{b,LTC} + \sum_{t=1}^{T}\left(q_t^{b,SPM+} - q_t^{b,SPM-}\right) - \sum_{t=1}^{T} d_t = 0 \quad (\rho^b), \tag{9.c}$$

where Q^b represents the importer's regasification capacity, which is constant at each delivery time t. $ord(T)$ denotes the ordinal number of T in the sequential set $\{1,2,\dots,T\}$. $\frac{q^{b,LTC}}{ord(T)}$ represents the LTC LNG delivered at each t. d_t indicates the demand of gas consumption at t. λ_t^b, μ_t^b and ρ^b are the shadow prices of corresponding constraints. As the importer is a price taker, $\tilde{p}_t^{SPM}$, $\tilde{p}^{LTC}$ and $\tilde{f}_t^{SPM}$ (contained in $\tilde{\pi}^b$—see Section 3.2) can be regarded as given. The decision variables in this optimization problem are $q^{b,LTC}$, $q_t^{b,SPM+}$ and $q_t^{b,SPM-}$. Constraint (9.a) expresses that the total import volume of LNG should be restricted by the importer's regasification capacity. In constraint (9.b), the term $\frac{q^{b,LTC}}{ord(T)} + q_t^{b,SPM+} - q_t^{b,SPM-}$ indicates the net procurement volume of importer at t. $(ord(t)-1)\frac{q^{b,LTC}}{ord(T)} + \sum_{t'<t}\left(q_{t'}^{b,SPM+} - q_{t'}^{b,SPM-} - d_{t'}\right)$ indicates the LNG inventory up to t. Constraint (9.b) ensures that, at each delivery time t before settlement of the LTC, the sum of net procurement and inventory should at least satisfy gas consumption. Constraint (9.c) is the special case of Constraint (9.b), when t equals T. Constraint (9.c) is stricter, however, so as to ensure market clearing within the gas consumption market. This constraint implies that the total net LNG procurement of the importer should be equal to consumption during the trading period.

The utility maximization of the exporter is given as:

$$\max_{q^{s,LTC}} \mathbb{E}[U(\tilde{\pi}^s)] \tag{10}$$

Subject to

$$q^{s,LTC} + \sum_{t=1}^{T} q_t^{s,SPM} \leq Q^s \ \ (\lambda^s), \tag{10.a}$$

where Q^s is the exporter's production capacity during the trading period, and λ^s is the shadow price of constraint (10.a). As the exporter is also a price taker, $\tilde{p}_t^{SPM}$ and $\tilde{p}^{LTC}$ (contained in $\tilde{\pi}^s$) are treated as given. In this study, we assume that $\tilde{p}_t^{SPM}$ is an equilibrium price, which implies that the spot volume sold by the exporter ($q_t^{s,SPM}$) is dependent on the demand of the importer. Therefore, the decision variable in this optimization problem is only the LTC volume sold by the exporter ($q^{s,LTC}$). Due to oversupply in the LNG market (Sesini et al., 2020), we assume that the exporter can satisfy the demand of the importer at each delivery time t. Hence, we do not impose the restriction on the LNG exports during each delivery period. Constraint (10.a) only ensures that the total LNG exports in the trading period are not greater than Q^s.

We introduce the **market clearing conditions** as follows:

$$q^{b,LTC} = q^{s,LTC}, \tag{11}$$

which represents the equilibrium in LTC trade between a given importer and exporter. Additionally,

$$q_t^{b,SPM+} = q_t^{s,SPM}, \tag{12}$$

which indicates equilibrium in the spot market between the importer and the exporter. In order to solve this model, we transport it into a mixed complementarity problem (MCP), via the KKT conditions and market clearing conditions. A detailed description of the transformed MCP is given in Appendix A.

4. Simulation of stochastic inputs

Three random variables act as the stochastic inputs in the proposed equilibrium model: a) the oil price $\tilde{p}_t^{OIL}$; b) the LNG spot price (CIF) $\tilde{p}_t^{SPM}$; and c) the spot freight rate $\tilde{f}_t^{SPM}$. In this section, we apply historical data in order to simulate the movements of these three prices over a trading period from November, 2020 to December, 2021. In Section 4.1, we present the econometric approach for the simulation. In Section 4.2, we show the simulated results.

4.1 Simulation procedure of stochastic inputs

The purpose of simulating the aforementioned random prices is to determine the expectation $\mathbb{E}(\tilde{\pi}^h)$ and variance $Var(\tilde{\pi}^h)$ of each agent's profits in the equilibrium model. This requires that our approach not only forecast short-term price trends accurately, but also capture their distribution characteristics. To this end, we apply an approach that combines a mean-reversion model and kernel regression model.

We assume that three prices satisfy the mean reversion process. This model can be described as the following differential equation:

$$dz_t = \mu(m_t - z_t)dt + \sigma dW_t, \quad t = 1,2,\dots,T \tag{13}$$

where z_t is the logarithm of a price p_t. μ and σ are positive parameters reflecting the speed and volatility of mean reversion, respectively. m_t is the time-dependent mean of z_t. W_t represents a Wiener process. By following Gersema and Wozabal (2018), we apply a locally constant kernel regression to estimate m_t. The regression function is given as:

$$m_t = E[z|F(t)] = \frac{\sum_{\tau=1}^{T} K_h[F(t) - F(\tau)]z_\tau}{\sum_{\tau=1}^{T} K_h[F(t) - F(\tau)]}, \qquad t,\tau \in [0,1,2,\dots,T] \tag{14}$$

where $K_h(\cdot)$ is a Gaussian kernel with h bandwidth, $F(t)$ denotes the time transformation, representing the periodic characteristic of prices, such as seasonality. If there is no clear periodicity in the price series, $F(t)$ can directly equal $ord(t+1)$[2]. In order to estimate the parameters μ and σ, we refer to the approach of Tseng and Barz (2002), who constructed a mean reversion process for a stationary series by removing the periodicity and trends from the price series.

First, we remove the periodicity of z_t, and obtain the logarithm price without periodicity, $\dot{z}_t$. We define the periodicity as monthly. This periodicity can be represented as the difference between the average logarithm price of the month, and the average logarithm price over the sample period. For example, given a sample period from 2010 to 2019, the mean of all January logarithm prices minus the average logarithm price over 10 years is equal to the periodicity of January.

Second, we construct the stationary price series $\ddot{z}_t$ by detrending $\dot{z}_t$. We define the trend of $\dot{z}_t$ as being yearly. The trend is represented by the difference between the annual mean of $\dot{z}_t$ and the mean of $\dot{z}_t$ over the sample period.

Last, we display the mean reversion process for the modified price series $\ddot{z}_t$ as follows:

$$d\ddot{z}_t = \mu(m - \ddot{z}_t)dt + \sigma dW_t, \quad t = 1,2,\dots,T \tag{15}$$

[2] $ord(t+1)$ indicates the ordinal number of t in the ordered set $\{0,1,2,\dots,T\}$.

where m is the mean of $\ddot{z}_t$. Note that m is time invariant, since the price series $\ddot{z}_t$ is stationary. For the purposes of parameter estimation, we transform equation (15) into the following, discrete-time form:

$$\ddot{z}_t - \ddot{z}_{t-1} = [1 - \exp(-\mu)](m - \ddot{z}_{t-1}) + \epsilon_t, \ \ t = 1,2,\dots,T \tag{16}$$

where the residual ϵ_t should be subject to $N(0, {\sigma_\epsilon}^2)$. Based on equation (16), we fit time series $\ddot{z}_t$, using the maximum likelihood approach. The corresponding maximum likelihood estimators are shown as:

$$\begin{aligned} m &= \frac{1}{ord(T)} \sum_{t=0}^{T} \ddot{z}_t - \frac{1}{ord(T)} \frac{\ddot{z}_0 - \exp(-\mu)\, \ddot{z}_t}{1 - \exp(-\mu)} \\ &\approx \frac{1}{ord(T)+1} \sum_{t=0}^{T} \ddot{z}_t\,, \ \ for\ \ddot{z}_0, \ddot{z}_T \approx m, \end{aligned} \tag{17}$$

$$\mu = -\ln\left[\frac{\sum_{t=1}^{T}(\ddot{z}_t - m)(\ddot{z}_{t-1} - m)}{\sum_{t=1}^{T}(\ddot{z}_{t-1} - m)^2}\right], \tag{18}$$

$${\sigma_\epsilon}^2 = \frac{1}{ord(T)} \sum_{t=1}^{T} [(\ddot{z}_t - m) - \exp(-\mu) \cdot (\ddot{z}_{t-1} - m)]^2, \tag{19}$$

$$\sigma^2 = \frac{2\mu {\sigma_\epsilon}^2}{1 - \exp(-2\mu)}. \tag{20}$$

Note that, in equation (17) and (19), $ord(T)$ indicates the ordinal number of T in the ordered set.

After estimating parameters μ and σ, we substitute them into the time-varying process. The original logarithm price z_t can then be simulated as:

$$z_t = [1 - \exp(-\hat{\mu})]m_{t-1} + \exp(-\hat{\mu})\, z_{t-1} + \varepsilon_t, \ \ t = 1,2,\dots,T \tag{21}$$

where the residual ε_t should be subject to $N(0, \hat{\sigma}^2)$, $\hat{\mu}$ and $\hat{\sigma}$ denote the estimated results of the parameters via the maximum likelihood approach. As we have determined the distribution characteristics of ε_t, we apply the Monto Carlo approach in order to generate scenarios of p_t. The corresponding steps are shown as:

- First, we generate I ($I = 5000$) scenarios for each ε_t. The scenarios of ε_t can be aggregated as a vector $\boldsymbol{\varepsilon_t} = [\varepsilon_{1t}, \varepsilon_{2t}, \dots, \varepsilon_{it}, \dots, \varepsilon_{It}]^T$.
- Second, the price movement $\boldsymbol{z_i} = [z_{i1}, z_{i2}, \dots, z_{it}, \dots, z_{iT}]^T$ in each scenario i can be simulated using equation (21), via substituting ε_t with ε_{it}.
- Third, repeat the second step for all scenarios. Scenarios of each z_t should be

the vector $\boldsymbol{z_t} = [z_{1t}, z_{2t}, \dots, z_{it}, \dots, z_{It}]^T$. Scenarios of p_t are defined as the vector $\boldsymbol{p_t}$, where $\boldsymbol{p_t} = \exp(\boldsymbol{z_t})$.

Within the scenario vector $\boldsymbol{p_t}$, we can further estimate expectations and covariance matrices over the three random prices, which act as the stochastic inputs of the equilibrium model.

4.2 Simulated results

In this section, we present the simulated results for each of the stochastic inputs into the equilibrium model, that is, the oil price, the LNG spot price, and the spot freight rate.

The oil price in the equilibrium model represents one choice for an LTC pricing benchmark. In this study, we adopt the Japan Crude Cocktail (JCC) price, which is a commonly used oil-indexed benchmark for LNG LTCs in Asia. The monthly data on JCC prices are published by the Ministry of Economy, Trade and Industry (METI) of Japan. The in-sample period ranges from January 2000 to October 2020. The out-of-sample period ranges from November 2020 to October 2021. The in-sample, real JCC price is shown as the blue line in Figure 3 (a). Since it does not have obvious periodicity, we apply $ord(t+1)$ as the time transformation $F(t)$ for kernel regression. In order to provide a basis for the out-of-sample forecast, we use the observed JCC futures prices on October 29, 2020 to profile the trend of mean reversion from November 2020 to October, 2021. This analysis is shown as a black line in Figure 3 (a). By incorporating the in-sample, real JCC price, we form a 2000-2021 time series that acts as the input of kernel regression, so as to keep the continuity of estimation. The estimation result of the time-dependent mean from the kernel regression is shown in Figure 3 (a) as a red line. The estimated parameters $\hat{\mu}$ and $\hat{\sigma}$ for the JCC price are 0.390 and 0.094 (see Table 1). We use R^2 and Mean Absolute Percentage Error (MAPE) to examine the fit performance of the previously described approach to in-sample data. As shown in Table 1, the R^2 and MAPE in the JCC price simulation are 0.974 and 0.025, respectively. This indicates that the estimated result is a good fit for the real data in the in-sample period. Then, we forecast the JCC price over the out-of-sample period. Figure 4 (a) displays the forecast result over a 95% confidence level.

The JKM price is an alternative choice for replacing the oil-indexed benchmark. The weekly data is sourced from Thomson Reuters Eikon. The in-sample period ranges from July 31, 2014 to October 29, 2020. The out-of-sample period ranges from November 5, 2020 to October 30, 2021. In Figure 3 (b), the blue line shows the real JKM price during the in-sample period. Similar to the JCC price, the JKM price doesn't show obvious periodicity. We therefore set the time transformation $F(t)$ as $ord(t+1)$ for kernel regression. The black line shows the JKM futures prices on October 29, 2020. The JKM futures prices make up a continuous time series together with the real JKM price for the time-dependent mean estimation. The red line in Figure 3 (b) represents the estimated, time-dependent mean of the JKM price from kernel regression. The estimated parameters $\hat{\mu}$ and $\hat{\sigma}$ for the JKM price mean-reversion process are 0.390 and 0.094. R^2 and MAPE are 0.976 and 0.031, respectively, showing that the estimated JKM price during the in-sample period is well fitted to the real data. Then, we forecast the JKM price over the out-of-sample period. Figure 4 (b) displays the forecast result over a 95% confidence level.

The spot freight rate is the trade cost item we are most concerned with in the model. In this paper, we use the spot freight rate from Baltic LNG Route 1 (BLNG1) as an example.[3] The in-sample weekly data between January 5, 2018 and October 29, 2020 is sourced from the Shipping Intelligence Network. The out-of-sample period ranges from November 5, 2020 to October 30, 2021. In Figure 3 (c), the blue line shows the real spot freight rate during the in-sample period. Unlike the JCC and JKM prices, the spot freight rate has obvious periodicity. Briefly, the spot freight rate maintains an upward trend from April to October. The freight rate displays a downward trend from October to April of the following year. The periodicity of the spot freight rate leads to a different time transformation $F(t)$, shown as:

$$F(t) = \sin\left(\pi + \frac{ord(t+1)}{26}\pi\right) + ord(t+1), \tag{22}$$

where $\sin\left(\pi + \frac{ord(t+1)}{26}\pi\right)$ indicates the stationary periodicity in the long run. The black line shows the BLNG1 futures prices observed in the Thomson Reuters Eikon on October 29, 2020. These prices act as the trend for the mean reversion in the out-of-sample period. The real prices and the related futures prices together construct the time series for the time-dependent mean of sport freight rate. The estimated time-dependent mean is shown as the red line in Figure 3 (c). The estimated parameters $\hat{\mu}$ and $\hat{\sigma}$ for the spot freight rate mean-reversion process are 0.259 and 0.211. R^2 and MAPE are 0.943 and 0.011, respectively, showing that the estimated spot freight rate during the in-sample period is well fitted with the real data. Figure 4 (b) displays the out-of-sample forecast result over a 95% confidence level.

Table 1. In-sample fit of estimated prices compared to real data.

	$\hat{\mu}$	$\hat{\sigma}$	R-squared	MAPE
JCC	0.390	0.094	0.974	0.025
JKM	0.095	0.080	0.976	0.031
Spot freight rate	0.259	0.211	0.943	0.011

[3] Baltic LNG route 1 (BLNG1) refers to the route between Gladstone (Australia) and Tokyo (Japan).

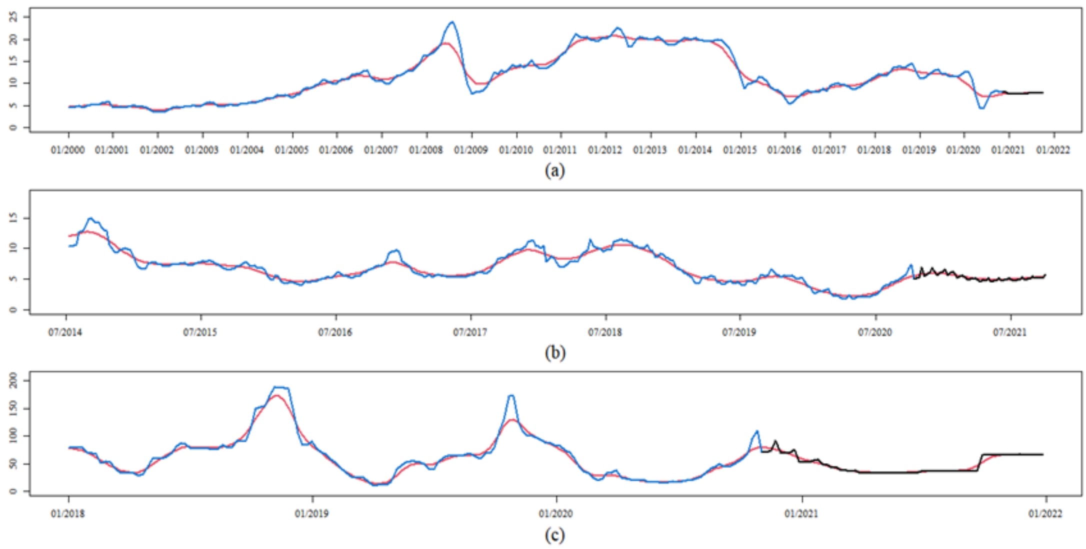

Fig. 3. Estimated results of time-dependent mean (m_t).

Note: Panels (a), (b), and (c) show the time-dependent mean of the JCC price, the JKM price and the spot freight rate, respectively. The x-axis indicates the whole estimation period, while the y-axis indicates the price. The Red line represents the time-dependent mean. The Blue line represents the real price during the in-sample period. The Black line represents the price of futures, which will mature during the out-of-sample period. The unit of both the JCC and the JKM price is \$/MMBtu. The unit of spot freight rate is thousand \$/day.

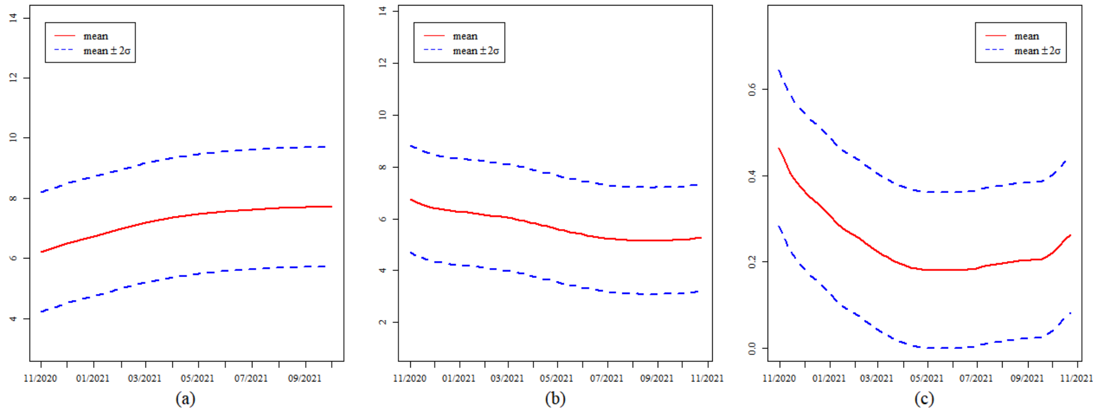

Figure 4. Forecast prices during out-of-sample period (unit: \$/MMBtu).

Note: Panels (a), (b), and (c) show the forecast results of the JCC price, the JKM price, and the spot freight rate, respectively.[4] The x-axis indicates the out-of-sample period, and the y-axis indicates the price (\$/MMBtu).

[4] We unify the unit of the spot freight rate with the unit of other prices as \$/MMBtu. The unit of original data on the spot freight rate is thousand \$/day. As reported by Baltic Exchange, the voyage cycle of the BLNG 1 route is around 26 days (including port waiting time). A standard LNG tanker on this route can carry approximately 160 thousand cubic meters (5.853 million MMBtu) of LNG. Thus, one thousand \$/day can be equally converted to $\frac{26}{5853}$ \$/MMBtu. All of the information on the BLNG 1 route is available at https://www.balticexchange.com/en/data-services/routes.html

5. Results

Based on the price forecast results in Section 4, we conduct a case study in this section in order to evaluate the efficiency of the three different benchmarks for LTC pricing, and the risk-profit tradeoffs for the importer and the exporter. The case study we have chosen is a trade between a Japanese importer and an Australian exporter. They sign an LTC on October 29, 2020. The first settlement of the LTC will be conducted on October 30, 2021. According to the terms of the LTC, gas will be delivered in equal volumes on a weekly basis. In order to account for the seasonality of LNG consumption, we assume that the peak season consists of two periods: a) the period from the 1st week up to the 12th week after October 29, 2020; b) the period from the 40th week to the 52nd week. The slack season begins from the 13th week to 39th week after October 29, 2020.

The detailed information related to the parameters of the equilibrium model is shown in Table 2. As for the risk aversion parameter γ^h, we estimate that its order of magnitude is 10^{-2}. The exporter's risk aversion parameter γ^s is three times that of the importer's, denoted by γ^b. A detailed discussion of the risk aversion parameter is shown in Appendix B. In the following study, we will treat γ^h as a range between $10^{-3.5}$ to $10^{0.5}$, based on its order of magnitude. With this range, a risk aversion-based sensitivity analysis will be conducted in order to understand the effect of various risk aversion levels.

Table 2. Value of parameters in the model

Parameters	Value
$\sum_{t=1}^{T} d_t$	150 million MMBtu[5]
$\bar{p}^{CPM}$	9 \$/MMBtu
Q^s	300 million MMBtu
Q^b	7.212 million MMBtu per week[6]
d_t in the peak season	4 million MMBtu per week
d_t in the slack season	1.852 million MMBtu per week

5.1 Trade volume and LTC based price

We first analyze how LTC and spot trade volumes change with a given agent's risk aversion. Figure 5 (a), (b), and (c) present the impact of risk aversion on the LTC and spot trade volumes. Generally, the results suggest that the change trend of LTC and spot trade volumes under the oil price benchmark are consistent with those observed under

[5] We assume that this importer is a small gas retailer. In 2020, Japanese LNG imports were 3.67 billion MMbtu (UN Comrade, 2020). This retailer only takes up 4% of the shares in the Japanese consumption market.

[6] As reported by the U.S. Energy Information Administration, the annual regasification capacity of Japan in 2020 was 10 billion MMbtu, which is 2.7 times the level of Japanese LNG imports. Here we set 2.5 times the importer's domestic supply (150 million MMbtu) as its annual regasification capacity. Equivalently, the weekly regasification capacity is 7.212 million MMbtu.

the JKM price benchmark. LTC dominates the trade between importer and exporter when risk aversion is relatively low. The importer resells the LNG as much as possible within the spot market while meeting the demand of the consumer market. With an increase in risk aversion, the proportion of spot trade volume begins to increase, and eventually dominates the LNG trade. At the same time, the importer's resale in the spot market keeps declining.

The difference in trade volumes among different benchmarks is that the oil-indexed LTC volume is less sensitive to the agents' levels of risk aversion. As shown in Figure 5 (a), when the risk aversion increases from -3 to -2.5, the oil-indexed LTC volume remains 300 million MMBtu, but the JKM-indexed LTC declines to 260 million MMBtu. When the risk aversion ranges from -1.75 to 0.5, the JKM-indexed LTC is absent, but the oil-indexed LTC remains. In addition, the low sensitivity of the oil-indexed LTC to risk aversion leads to low spot trade volume. From Figure 5 (b) and (c), we can find that the spot trade volume between the importer and the exporter (as well as the importer's spot resale) under the oil price benchmark is less than the volume traded under the JKM price benchmark. This indicates that using the JKM price as the LTC pricing benchmark can promote the LNG spot trade.

Figure 5 (d) shows the relationships between the base price of the LTC and the risk aversion. We can observe that the base price of the LTC is significantly different among the three benchmarks. The base price of the oil-indexed LTC turns out to be very high when risk aversion is larger than -0.5. With a risk aversion of 0.5, it reaches the highest value of 55 \$/MMBtu. The base price of the JKM-indexed LTC remains stable, however, with a slight decline from 7.11 (6.3) \$/MMbtu to 6.5 (5.9) \$/MMbtu in the CIF (FOB) case.

The results of the LTC's base price provide an intuitive judgment, that is, the JKM price is more efficient as an LTC pricing benchmark compared to the oil price. The reason is that the JKM-indexed LTC performs better in risk-sharing. For an ideal LTC with the perfect risk-sharing, the TOP clause should fully impose the price risk on the exporter. This implies that the base price should be a risk-neutral price expectation, which is essentially a reflection of the total supply and demand in the market. In terms of the assumption that both the importer and the exporter are price takers, any change in risk aversion should not affect the price expectation. Apparently, the base price of the JKM-indexed LTC is more in line with the criteria of a stable risk-neutral expectation.

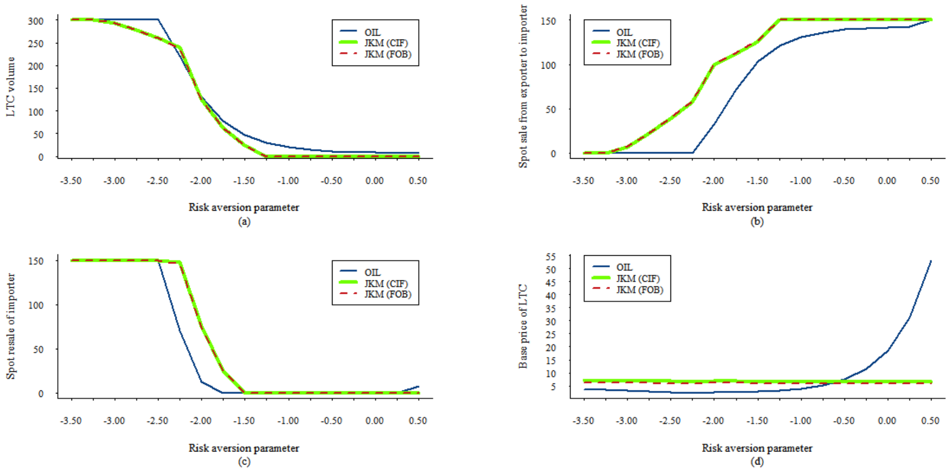

Figure 5. LNG trade volumes and base price of LTC under different levels of risk aversion.

Note: Panel (a) shows the LTC volumes. Panel (b) shows the spot LNG sales from the exporter to the importer. Panel (c) shows the spot resales of the importer. Panel (d) shows the base price of the LTC. The x-axis indicates the risk aversion parameter γ^h, which is denoted as $\log \gamma^h$. Given a certain γ^h, the risk aversion parameter of importer γ^b is equal to γ^h, and that of exporter γ^s is $3\gamma^h$. The unit of the y-axis in panels (a), (b), and (c) is million MMBtu. The unit of y-axis in panel (d) is \$/MMBtu.

5.2 Hedging position and hedging effectiveness

We next discuss the hedging function of LTCs priced under different benchmarks. While analyzing the LTC base price, we find that TOP clauses under any benchmark cannot perfectly share the risks between counterparties. This can be evidenced by the fact that the base price still changes with risk aversion, even when using the JKM as the benchmark. This result is consistent with reality, as no price benchmark can perfectly reflect supply and demand in the market. This also means that the exporter does not completely bear the price risk. Specifically, the base price contains the risk compensation for the exporter, resulting in a part of the price risk being transferred to the importer. Hence, the role of the LTC as a hedging instrument becomes critical to the importer. Suppose that an importer resells an amount of LNG while purchasing an LTC. These two opposite transactions will form a hedging instrument so as to offset the transferred price risk from the exporter, thereby ensuring that the risk-sharing function of the LTC remains in place. Therefore, it is of practical significance to discuss benchmark efficiency from the perspective of an LTC's hedging function.

According to the KKT conditions of the importer's optimization problem in the equilibrium model, we can get the following expression with regard to LTC purchasing volume of a given importer ($q^{b,LTC}$):

$$q^{b,LTC} = \frac{\bar{p}^{CPM} - E\left(\tilde{p}^{LTC} + (1-\kappa)\bar{f}^{LTC}\right) - \sum_{t=1}^{T} \lambda_t^b - \rho^b + \sum_{t=1}^{T-1} \mu_t^b}{\gamma^b \cdot Var\left(\tilde{p}^{LTC}\right)} + \tag{23}$$

$$\sum_{t=1}^{T} \frac{-q_t^{b,SPM+} Cov(\tilde{p}^{LTC}, \tilde{p}_t^{SPM}) + q_t^{b,SPM-} Cov(\tilde{p}^{LTC}, \tilde{p}_t^{SPM} - \tilde{f}_t^{SPM})}{Var(\tilde{p}^{LTC})}, \ if \ q^{b,LTC} > 0.$$

On the right-hand side of equation (23), the first term indicates the speculative position of the LTC, and the second term represents the hedging position. $\frac{Cov(\tilde{p}^{LTC}, \tilde{p}_t^{SPM})}{Var(\tilde{p}^{LTC})}$ and $\frac{Cov(\tilde{p}^{LTC}, \tilde{p}_t^{SPM} - \tilde{f}_t^{SPM})}{Var(\tilde{p}^{LTC})}$ are the best hedging ratios for importer to hedge its spot resales ($q_t^{b,SPM-}$) and spot purchase from the exporter ($q_t^{b,SPM+}$), respectively. It should be noted that an LTC is different from futures or forward contracts. The unidirectionality of an LTC (only the exporter sells the LTC to the importer) determines that the importer can never hold a short position. This implies that the hedging of an LTC against spot trades is not complete for the importer. Equation (23) shows us that the necessary condition to form hedging between the LTC and a spot trade is that both LTC volume and the hedging position are positive. This can be further split into two conditions: a) when the LTC pricing benchmark is negatively correlated with the spot price, the hedging position against $q_t^{b,SPM+}$ should be larger than that against $q_t^{b,SPM-}$; b) when the benchmark is positively correlated with the spot price, the hedging position against $q_t^{b,SPM+}$ should be smaller than that against $q_t^{b,SPM-}$. Based on the price forecast results in Section 4, $Cov(\tilde{p}^{LTC}, \tilde{p}_t^{SPM})$ and $Cov\left(\tilde{p}^{LTC}, \tilde{p}_t^{SPM} - \tilde{f}_t^{SPM}\right)$ are negative in most cases under the oil price benchmark, and are positive under the JKM price benchmark (see Appendix C). In order to construct a hedge between the LTC and the spot trade, the importer should ensure that condition a) is met while using the oil price benchmark, or that condition b) is met while using the JKM price benchmark. We have displayed the importer's hedging positions in an LTC and the corresponding hedging effectiveness in Figure 6 (a) and (b), respectively.

Figure 6 (a) describes the relationship between the importer's hedging position and the agents' risk aversion. We can observe that the oil-indexed LTC offers a hedging position under a high level of risk aversion (from -1.75 to 0.5), and that the JKM-indexed LTC offers a hedging position under a low level of risk aversion (from -3.75 to -1.75). This result verifies the incomplete hedging instrument that the LTC is.

More importantly, for a spot trade of the same scale, the oil-indexed LTC provides fewer hedging positions than the JKM-indexed one. For example, when the risk aversion parameter is 0.5, the importer's net spot trade volume is 142.7 million MMBtu (a positive value indicates a purchase) under the oil price benchmark. When the risk aversion parameter is -3, the importer's net spot trade volume is -142.9 million MMBtu (a negative value indicates a sale) under the JKM FOB benchmark. Although the importer has the same spot trade scale in each of the two cases, the oil-indexed LTC provides 1.3 million MMBtu, while the JKM FOB provides 62.2 million MMBtu as the hedging position. The reason for this result is that the best hedge ratios under the oil price benchmark are much smaller than those under the JKM FOB benchmark. As the variance of LTC price $Var(\tilde{p}^{LTC})$ between two benchmarks is close (i.e., 0.99 for an oil-indexed LTC, and 1.07 for the JKM FOB-indexed one), the smaller absolute value of covariance $Cov(\tilde{p}^{LTC}, \tilde{p}_t^{SPM})$ and $Cov(\tilde{p}^{LTC}, \tilde{p}_t^{SPM} - \tilde{f}_t^{SPM})$ under the oil price benchmark (see Appendix C) leads to a smaller optimal hedge ratio. The difference in the covariance further indicates that there is a lack of correlation between the oil price and the spot LNG price.

Figure 6 (b) shows the relationship between hedging effectiveness (HE) of an LTC and risk aversion. The HE is defined as the reduction of spot trade risk though the introduction of hedging positions (Cotter and Hanly, 2012):

$$HE = -\frac{SD(spot\ return + return\ from\ Hedge\ position) - SD(spot\ return)}{SD(spot\ return)} \quad (24)$$

Under a low level of risk aversion (from -3.5 to -1.75), the JKM-indexed LTC can construct an effective hedging portfolio with spot trades for the importer. The maximum HE (64%) is reached at a risk aversion level of -2.25. As risk aversion is larger than -2.25, the HE of the JKM-indexed LTC decreases. This can be explained by the decrease in both LTC volume and in the importer's spot resale. This result implies that the demand for risk hedging is reduced as the importer significantly increases spot purchases from the exporter in order to satisfy domestic consumption. As risk aversion increase from -1.75, the HE declines to zero, as no LTC exists under the JKM benchmark. As for the oil price benchmark, the HE of the LTC is almost zero. This result indicates that the oil-indexed LTC is ineffective in providing hedging for the importer. These results confirm that JKM price is more efficient than the oil price as the benchmark for LTC pricing, as the JKM-indexed LTC can be an effective hedging instrument for the importer.

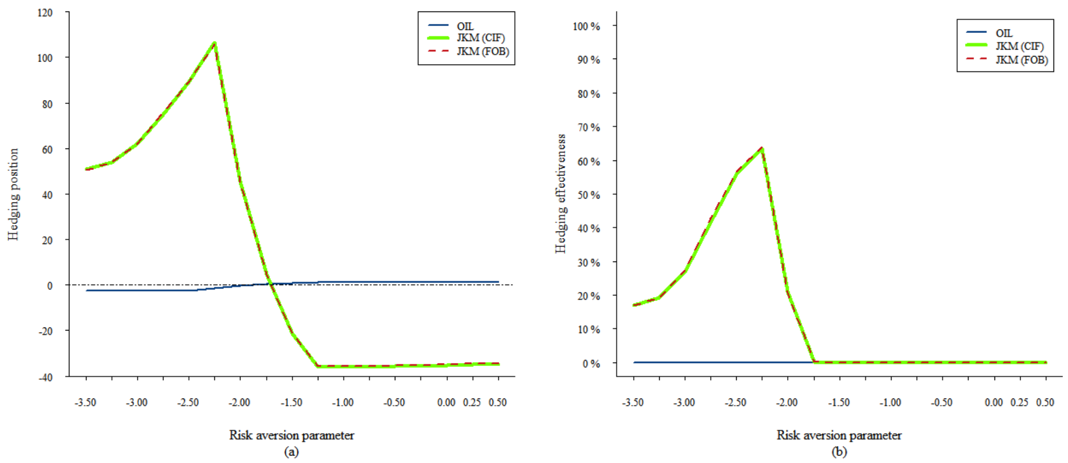

Figure 6. Importer's hedging position on an LTC and hedging effectiveness.

Note: Panel (a) describes the hedging position, and panel (b) describes the effectiveness of the hedging position. The x-axis indicates the risk aversion parameter γ^h, which is denoted as $\log \gamma^h$. Given a certain γ^h, the risk aversion parameter of importer γ^b is equal to γ^h, and that of exporter γ^s is $3\gamma^h$. The unit of the y-axis in panel (a) is million MMBtu.

5.3 Tradeoff between profits and risks

The previous two sections describe the JKM price as an efficient benchmark for LTCs. In this section, we will explore whether this benchmark is feasible. The adoption of this pricing measure relies on whether the benchmark can improve profit and lower the corresponding risks of the importer and exporter. In this study, we apply the coefficient of variance (CV) to represent the tradeoffs for the importer and the exporter between expected profit and profit-related risk. A smaller CV implies a better risk-profit tradeoff for both the importer and the exporter.

Figure 7 (a) and (b) show the change in CV of the importer and the exporter respectively. In the risk aversion range between -3.5 and -1.75 (low risk aversion), the CV of an importer under the JKM benchmark is always less than that under the oil price benchmark. For the exporter, the JKM benchmark also preforms better than the oil price benchmark in most cases. This indicates that the JKM benchmark is beneficial to both the importer and the exporter under conditions of low risk aversion. This is because, on the one hand, the JKM benchmark contributes to a higher LTC base price—which helps the exporter to transfer more price risk onto the importer. On the other hand, the JKM benchmark provides an effective hedging mechanism for the importer to offset the transferred price risk.

In the risk aversion range between -1.75 and -0.5 (moderate risk aversion), the oil price performs better than the JKM price as a benchmark of LTC pricing, since the CV of the importer and the exporter under the oil price benchmark is less than under the JKM benchmark. The reason for this is that the JKM-indexed LTC cannot provide effective hedging, although the LTC volume exists. This result implies that the JKM-indexed LTC is similar to the oil-indexed one, and should be viewed as an option within an LNG trade portfolio for risk diversification. It is known that less correlated assets among a portfolio perform better in risk diversification. Therefore, the oil price is the better choice for LTC pricing in this case.

In the risk aversion range between -0.5 and 0.5 (high risk-aversion), the CV of the importer under the JKM benchmark is significantly smaller than that under the oil price benchmark. The oil price benchmark, however, is more favorable for the exporter. The reason for this is that the JKM-indexed LTC is zero, while that a few amounts of oil-indexed LTC still exist. It implies that oil-indexed LTC is available to transfer exporter's price risks while JKM-indexed one is not. With this high risk-averse attitude, the exporter needs to transfer more price risks, thereby driving a drastic increase in the base price of the oil-indexed LTC. As the oil-indexed LTC cannot provide an effective hedging option for the importer, the LTC that the importer purchased becomes an expensive sunk cost, which leads to profit losses for the importer.

Overall, these results show that the choice of an LTC pricing benchmark depends on the risk aversion of both the importer and the exporter. The JKM benchmark can benefit both the importer and the exporter under low levels of risk aversion. The oil price benchmark can be more suitable for both parties under conditions of moderate risk aversion (-1.75 ~ -0.5), due to its better risk diversification. Notably, the oil price benchmark is significantly inefficient to price the LTC in the high risk-aversion case (-0.5 ~ 0.5). Due to the decoupling of oil prices and the LNG spot price, the risk-sharing function of the oil-indexed LTC fails, and instead becomes a tool for the exporters to transfer price risk. The high risk-aversion of the exporter results in a high base price of the LTC, under which, the importer bears expensive gas-importing costs. For the importer, the essence of building an efficient pricing benchmark is to prevent the transfer of price risk. From this perspective, using the JKM price as the LTC pricing benchmark is helpful.

In addition, we find that there is no obvious difference in LNG trade volumes, base prices, or hedging effectiveness of LTCs when using either the JKM CIF price or using the JKM FOB price as the benchmark. The freight liability transferred from the exporter to the importer has little effect on the pricing efficiency. Consequently, we can conclude that the freight rate is not a determining factor in influencing price transparency.

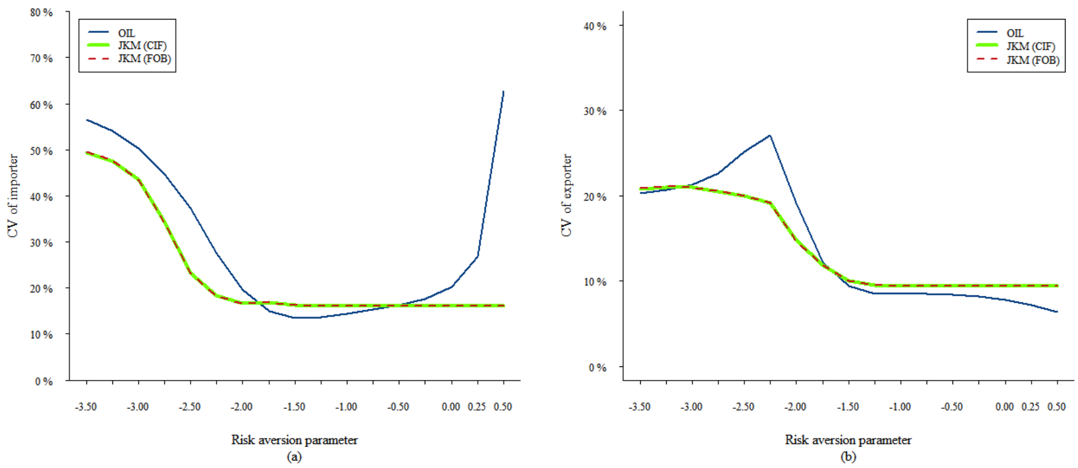

Figure 7. Coefficient of variance (CV) of expected profit under different levels of risk aversion.

Note: Panel (a) describes the CV of a given importer's expected profit, and panel (b) describes the CV of the exporter's expected profit. The x-axis indicates the risk aversion parameter γ^h, which is denoted as $\log \gamma^h$. Given a certain γ^h, the risk aversion parameter of importer γ^b is equal to γ^h, and that of exporter γ^s is $3\gamma^h$.

6. Conclusion

In this paper, we have established an LTC pricing equilibrium model that considers the risk aversion of an Asian LNG importer and an exporter, as well as price uncertainties. As an extension of the mean-variance utility framework, we highlight that a) natural gas is storable; and, b) the Asian LNG is traded at the CIF price. Based on the mean-reversion model and the kernel regression model, we forecast uncertain prices and capture their distributional characteristics. Finally, we simulate the corresponding stochastic inputs (that is, price expectation and covariance matrices) of the equilibrium model via the Monte Carlo method.

Using the equilibrium model, we conduct a risk aversion-related sensitivity analysis and make a comparison between the oil price and the JKM price in order to analyze their performance as a benchmark for pricing the LTC of Asian LNG. Our results are consistent with the conclusion from studies on oil-gas price nexus that the JKM price is suitable for serving as the pricing benchmark for LTC contracts in Asia. On top of this, we further find the JKM-indexed LTC can prevent the price risk transfer from an exporter to an importer. This demonstrates that introducing the JKM benchmark can benefit the Asian LNG importer. More importantly, we reveal that the risk attitudes of importer and exporter together determine the type of pricing benchmark, namely, JKM price and oil price. Therefore, a single pricing benchmark will limit the opportunities for them to find the consensus in pricing benchmark selection. The coexistence of JKM benchmark and oil indexation can benefit the Asian LNG trade.

Along with the increasing data availability in the future, this study can be extended in following two directions. The first direction is to consider LNG transactions involving multiple importers and exporters. The consideration for this line of study is that the assumption of agents in the gas market as price takers should be relaxed, since the unequal distribution of gas resources determines that some LNG exporters naturally have market powers. The second direction refers to the impact of freight rate on the LNG trade. In this study, we find that there is little effect on the trade, while the freight liability is transferred from the exporter to the importer. The possible reason for this result could be the exogenous freight rate in the model. This implies that the freight liability transfer is simplified as a trade cost transfer between the exporter and the importer. The influence from LNG carriers is neglected. Incorporating carriers' decisions into the model may bring different findings for us.

References

Abada, I., Ehrenmann, A. and Smeers, Y., 2017. Modeling gas markets with endogenous long-term contracts. *Operations research*, *65*(4), pp.856-877.

Alim, A., Hartley, P.R. and Lan, Y., 2018. Asian spot prices for LNG and other energy commodities. *The Energy Journal*, *39*(1).

Asche, F., Oglend, A. and Osmundsen, P., 2017. Modeling UK natural gas prices when gas prices periodically decouple from the oil price. *The Energy Journal*, *38*(2).

Ason, A., 2020. *Scenarios for Asian long-term LNG contracts before and after COVID-19*. Oxford Institute for Energy Studies.

Batten, J.A., Ciner, C. and Lucey, B.M., 2017. The dynamic linkages between crude oil and natural gas markets. *Energy Economics*, *62*, pp.155-170.

Bessembinder, H. and Lemmon, M.L., 2002. Equilibrium pricing and optimal hedging in electricity forward markets. *the Journal of Finance*, *57*(3), pp.1347-1382.

BP, 2020. BP statistical review of world energy 2020.

Brigida, M., 2014. The switching relationship between natural gas and crude oil prices. *Energy Economics*, *43*, pp.48-55.

Brown, S.P. and Yucel, M.K., 2008. What drives natural gas prices?. *The Energy Journal*, *29*(2).

Cotter, J. and Hanly, J., 2012. Hedging effectiveness under conditions of asymmetry. *The european Journal of finance*, *18*(2), pp.135-147.

Egging, R., Holz, F. and Gabriel, S.A., 2010. The World Gas Model: A multi-period mixed complementarity model for the global natural gas market. *Energy*, *35*(10), pp.4016-4029.

Egging, R., Pichler, A., Kalvø, Ø.I. and Walle–Hansen, T.M., 2017. Risk aversion in imperfect natural gas markets. *European Journal of Operational Research*, *259*(1), pp.367-383.

Erdős, P., 2012. Have oil and gas prices got separated?. *Energy Policy*, *49*, pp.707-718.

Feijoo, F., Huppmann, D., Sakiyama, L. and Siddiqui, S., 2016. North American natural gas model: Impact of cross-border trade with Mexico. *Energy*, *112*, pp.1084-1095.

Ftiti, Z., Tissaoui, K. and Boubaker, S., 2020. On the relationship between oil and gas markets: a new forecasting framework based on a machine learning approach. *Annals of Operations Research*, pp.1-29.

Geng, J.B., Ji, Q. and Fan, Y., 2016. The impact of the North American shale gas revolution on regional natural gas markets: Evidence from the regime-switching model. *Energy Policy*, *96*, pp.167-178.

Gersema, G. and Wozabal, D., 2017. An equilibrium pricing model for wind power futures. *Energy Economics*, *65*, pp.64-74.

Gersema, G. and Wozabal, D., 2018. Risk-optimized pooling of intermittent renewable energy sources. *Journal of banking & finance*, *95*, pp.217-230.

Guo, Y. and Hawkes, A., 2018. Simulating the game-theoretic market equilibrium and contract-driven investment in global gas trade using an agent-based method. *Energy*, *160*, pp.820-834.

Hartley, P.R., Medlock III, K.B. and Rosthal, J.E., 2008. The relationship of natural gas to oil prices. *The Energy Journal*, *29*(3).

Holz, F., Richter, P.M. and Egging, R., 2016. The role of natural gas in a low-carbon Europe: infrastructure and supply security. *The Energy Journal*, *37*(Sustainable Infrastructure Development and Cross-Border Coordination).

Li, Y., Chevallier, J., Wei, Y. and Li, J., 2020. Identifying price bubbles in the US, European and Asian natural gas market: Evidence from a GSADF test approach. *Energy Economics*, *87*, p.104740.

Lovcha, Y. and Perez-Laborda, A., 2020. Dynamic frequency connectedness between oil and natural gas volatilities. *Economic Modelling*, *84*, pp.181-189.

Neumann, A. and Von Hirschhausen, C., 2015. Natural gas: an overview of a lower-carbon transformation fuel. *Review of Environmental Economics and Policy*, *9*(1), pp.64-84.

Palti-Guzman, L., 2018. The Future of Asia's Natural Gas Market: The Need for a Regional LNG Hub. *asia policy*, *13*(3), pp.101-126.

Ramberg, D.J. and Parsons, J.E., 2012. The weak tie between natural gas and oil prices. *The Energy Journal*, *33*(2).

Sesini, M., Giarola, S. and Hawkes, A.D., 2020. The impact of liquefied natural gas and storage on the EU natural gas infrastructure resilience. *Energy*, *209*, p.118367.

Shi, X. and Shen, Y., 2021. Macroeconomic uncertainty and natural gas prices: Revisiting the Asian Premium. *Energy Economics*, *94*, p.105081.

Shi, X. and Variam, H.M.P., 2016. Gas and LNG trading hubs, hub indexation and destination flexibility in East Asia. *Energy Policy*, *96*, pp.587-596.

Shi, X. and Variam, H.M.P., 2017. East Asia's gas-market failure and distinctive economics—A case study of low oil prices. *Applied energy*, *195*, pp.800-809.

Stern, J., 2014. International gas pricing in Europe and Asia: A crisis of fundamentals. *Energy Policy*, *64*, pp.43-48.

Stern, J. and Imsirovic, A., 2020. A Comparative History of Oil and Gas Markets and Prices: is 2020 just an ex-treme cyclical event or an acceleration of the energy transition. *Energy Insight*, *68*.

Tseng, C.L. and Barz, G., 2002. Short-term generation asset valuation: a real options approach. *Operations Research*, *50*(2), pp.297-310.

Vivoda, V., 2014. Natural gas in Asia: Trade, markets and regional institutions. *Energy Policy*, *74*, pp.80-90.

Wang, T., Zhang, D. and Broadstock, D.C., 2019. Financialization, fundamentals, and the time-varying determinants of US natural gas prices. *Energy Economics*, *80*, pp.707-719.

Zhang, D. and Ji, Q., 2018. Further evidence on the debate of oil-gas price decoupling: A long memory approach. *Energy Policy*, *113*, pp.68-75.

Zhang, D., Shi, M. and Shi, X., 2018a. Oil indexation, market fundamentals, and natural gas prices: An investigation of the Asian premium in natural gas trade. *Energy Economics*, *69*, pp.33-41.

Zhang, D., Wang, T., Shi, X. and Liu, J., 2018b. Is hub-based pricing a better choice than oil indexation for natural gas? Evidence from a multiple bubble test. *Energy Economics*, *76*, pp.495-503.

Zhuang, J. and Gabriel, S.A., 2008. A complementarity model for solving stochastic natural gas market equilibria. *Energy Economics*, *30*(1), pp.113-147.

Appendices

Appendix A: Mixed complementarity problem of the equilibrium model

We present the mixed complementarity problem (MCP) of the proposed equilibrium model into in this Appendix. The MCP consists of KKT conditions of importer/exporter's optimization problem and the market clearing conditions.

The importer's KKT conditions are:

$$\begin{aligned}\forall\, q^{b,LTC},\ \ 0 \le q^{b,LTC}& \\ &\perp -\bar{p}^{CPM} + E(\tilde{p}^{LTC}) + (1-\kappa)\bar{f}^{LTC} + \gamma^b q^{b,LTC} Var(\tilde{p}^{LTC}) \\ &+ \gamma^b \sum_{t=1}^{T} \Big[q_t^{b,SPM+} Cov(\tilde{p}^{LTC}, \tilde{p}_t^{SPM}) \\ &- q_t^{b,SPM-} Cov\big(\tilde{p}^{LTC}, \tilde{p}_t^{SPM} - \tilde{f}_t^{SPM}\big)\Big] + \sum_{t=1}^{T} \frac{\lambda_t^b}{ord(T)} \\ &- \sum_{t=1}^{T-1} \frac{ord(t)\mu_t^b}{ord(T)} + \rho^b \ge 0\end{aligned} \tag{A1}$$

$$\begin{aligned}\forall\, q_t^{b,SPM+},\ \ 0 \le q_t^{b,SPM+}& \\ &\perp -\bar{p}^{CPM} + E(\tilde{p}_t^{SPM}) \\ &+ \gamma^b \big[q_t^{b,SPM+} Var(\tilde{p}_t^{SPM}) \\ &- q_t^{b,SPM-} Cov\big(\tilde{p}_t^{SPM}, \tilde{p}_t^{SPM} - \tilde{f}_t^{SPM}\big)\big] \\ &+ \frac{\gamma^b}{2} \Bigg[\sum_{t' \ne t} q_{t'}^{b,SPM+} Cov\big(\tilde{p}_t^{SPM}, \tilde{p}_{t'}^{SPM}\big) \\ &- \sum_{t' \ne t} q_{t'}^{b,SPM-} Cov\big(\tilde{p}_t^{SPM}, \tilde{p}_{t'}^{SPM} - \tilde{f}_{t'}^{SPM}\big)\Bigg] \\ &+ \gamma^b q^{b,LTC} Cov(\tilde{p}^{LTC}, \tilde{p}_t^{SPM}) + \lambda_t^b - \mu_t^b - \sum_{t'>t}^{T-1} \mu_{t'}^b + \rho^b \ge 0\end{aligned} \tag{A2}$$

$$\forall\, q_t^{b,SPM-},\;\; 0 \le q_t^{b,SPM-}$$
$$\begin{aligned}
&\perp \bar{p}^{CPM} - E\left(\tilde{p}_t^{SPM} - \tilde{f}_t^{SPM}\right) \\
&+ \gamma^b\left[q_t^{b,SPM-} Var\left(\tilde{p}_t^{SPM} - \tilde{f}_t^{SPM}\right)\right. \\
&\left.- q_t^{b,SPM+} Cov\left(\tilde{p}_t^{SPM}, \tilde{p}_t^{SPM} - \tilde{f}_t^{SPM}\right)\right] \\
&+ \frac{\gamma^b}{2}\left[\sum_{t' \ne t} q_{t'}^{b,SPM-} Cov\left(\tilde{p}_t^{SPM} - \tilde{f}_t^{SPM}, \tilde{p}_{t'}^{SPM} - \tilde{f}_{t'}^{SPM}\right)\right. \\
&\left.- \sum_{t' \ne t} q_{t'}^{b,SPM+} Cov\left(\tilde{p}_t^{SPM} - \tilde{f}_t^{SPM}, \tilde{p}_{t'}^{SPM}\right)\right] \\
&- \gamma^b q^{b,LTC} Cov\left(\tilde{p}^{LTC}, \tilde{p}_t^{SPM} - \tilde{f}_t^{SPM}\right) + \mu_t^b + \sum_{t'>t}^{T-1} \mu_{t'}^b - \rho^b \\
&\ge 0 \quad \forall t, t' \in \{1,2,\dots,T-1\}
\end{aligned} \tag{A3}$$

$$\forall\, \lambda_t^b,\;\; 0 \le \lambda_t^b \perp Q^b - \frac{q^{b,LTC}}{ord(T)} - q_t^{b,SPM+} \ge 0 \quad \forall t \in \{1,2,\dots,T\} \tag{A4}$$

$$\begin{aligned}
\forall\, \mu_t^b,\;\; 0 \le \mu_t^b \perp &\frac{q^{b,LTC}}{ord(T)} + q_t^{b,SPM+} - q_t^{b,SPM-} + (ord(t)-1)\frac{q^{b,LTC}}{ord(T)} \\
&+ \sum_{t'<t}\left(q_{t'}^{b,SPM+} - q_{t'}^{b,SPM-} - d_{t'}\right) - d_t \ge 0
\end{aligned} \tag{A5}$$

$$\forall\, \rho^b,\;\; free\ \rho^b \perp q^{b,LTC} + \sum_{t=1}^{T}\left(q_t^{b,SPM+} - q_t^{b,SPM-}\right) - \sum_{t=1}^{T} d_t = 0 \tag{A6}$$

The exporter's KKT conditions are:

$$\begin{aligned}
\forall\, q^{s,LTC},\;\; 0 \le q^{s,LTC}& \\
&\perp -E(\tilde{p}^{LTC}) + \kappa \bar{f}^{LTC} + \gamma^s q^{s,LTC} Var(\tilde{p}^{LTC}) \\
&+ \gamma^s \sum_{t=1}^{T} q_t^{s,SPM} Cov\left(\tilde{p}^{LTC}, \tilde{p}_t^{SPM} - \tilde{f}_t^{SPM}\right) + \lambda^s \ge 0
\end{aligned} \tag{A7}$$

$$\forall\, \lambda^s,\;\; 0 \le \lambda^s \perp Q^s - q^{s,LTC} - \sum_{t=1}^{T} q_t^{s,SPM} \ge 0 \tag{A8}$$

$$\begin{aligned}
\tilde{p}^{LTC} = p_0^{LTC} &+ \delta(\tilde{p}_T^{OIL} - \bar{p}_0^{OIL}) \\
&+ (1-\delta)\left[\left(\tilde{p}_T^{SPM} - \kappa \tilde{f}_T^{SPM}\right) - \left(\bar{p}_0^{SPM} - \kappa \bar{f}_0^{SPM}\right)\right]
\end{aligned} \tag{A9}$$

The market clearing conditions are:

$$\forall\, p_0^{LTC},\;\; free\ p_0^{LTC} \perp q^{b,LTC} - q^{s,LTC} = 0 \tag{A10}$$

$$\forall\ q_t^{b,SPM+},\ free\ q_t^{b,SPM+} \perp\ q_t^{b,SPM+} - q_t^{s,SPM} = 0 \tag{A11}$$

Appendix B: Estimation of importer/exporter's risk aversion parameter

According to Eq. (A1) and Eq. (A7) in Appendix A, we can derive the formulars to calculate the risk aversion parameter of importer (γ^b) and that of exporter (γ^s), which are as follows:

$$\gamma^b = \frac{\bar{p}^{CPM} - E(\tilde{p}^{LTC}) - (1-\kappa)\bar{f}^{LTC} - \sum_{t=1}^{T}\frac{\lambda_t^b}{ord(T)} + \sum_{t=1}^{T-1}\frac{ord(t)\mu_t^b}{ord(T)} - \rho^b}{q^{b,LTC}Var(\tilde{p}^{LTC}) + \sum_{t=1}^{T} q_t^{b,SPM+}Cov(\tilde{p}^{LTC},\tilde{p}_t^{SPM}) - \sum_{t=1}^{T} q_t^{b,SPM-}Cov(\tilde{p}^{LTC},\tilde{p}_t^{SPM} - \tilde{f}_t^{SPM})}, \tag{B1}$$

$$\gamma^s = \frac{E(\tilde{p}^{LTC}) - \kappa\bar{f}^{LTC} - \lambda^s}{q^{s,LTC}Var(\tilde{p}^{LTC}) + \sum_{t=1}^{T} q_t^{s,SPM}Cov(\tilde{p}^{LTC},\tilde{p}_t^{SPM} - \tilde{f}_t^{SPM})}, \tag{B2}$$

where $q^{b,LTC}$ and $q^{s,LTC}$ should be positive to ensure that the two equalities hold. Based on the market clearing conditions, $q^{b,LTC}$ equals to $q^{s,LTC}$, and $q_t^{b,SPM+}$ equals to $q_t^{s,SPM}$. Since $\tilde{p}^{LTC}$, $q^{b,LTC}$, $q_t^{b,SPM+}$, and $q_t^{b,SPM-}$ in the future are not observable, we cannot estimate an accurate value of γ^b and γ^s based on the Eq. (B1) and Eq. (B2). However, we can estimate the order of magnitude for γ^b and γ^s according to the actual situation in the current LNG market.

We assume that the LTC will go on with the oil-indexed pricing. On the basis of LTC-spot trade volume ratio reported by **GIIGNL Annual Report 2020**[7], we assume that the LTC volume possesses 70% and spot trade volume possesses 30% in the LNG transaction between the importer and the exporter. The importer does not resell LNG in the spot market. With this assumption, we can determine that $q^{b,LTC}$ ($q^{s,LTC}$) equals to 105 million MMBtu, $\sum_{t=1}^{T} q_t^{b,SPM+}$ ($\sum_{t=1}^{T} q_t^{s,SPM}$) equals to 45 million MMBtu, and $q_t^{b,SPM-}$ equals to 0.

As the oil price is less correlated with the LNG spot price (see Appendix C), we can ignore the term of $\sum_{t=1}^{T} q_t^{b,SPM+}Cov(\tilde{p}^{LTC},\tilde{p}_t^{SPM})$ in Eq. (B1) and the term of $\sum_{t=1}^{T} q_t^{s,SPM}Cov(\tilde{p}^{LTC},\tilde{p}_t^{SPM} - \tilde{f}_t^{SPM})$ in Eq. (B2). Without considering the constraints we set the model, γ^b and γ^s can be approximately estimated by following formulars:

$$\gamma^b \approx \frac{\bar{p}^{CPM} - E(\tilde{p}^{LTC})}{q^{b,LTC}Var(\tilde{p}^{LTC})}, \tag{B3}$$

$$\gamma^s \approx \frac{E(\tilde{p}^{LTC}) - \bar{f}^{LTC}}{q^{s,LTC}Var(\tilde{p}^{LTC})}. \tag{B4}$$

[7] GIIGNL Annual Report 2020 is available at https://giignl.org/system/files/publication/giignl_-_2020_annual_report_-_04082020.pdf/

We use the average LTC price during November, 2020 to replace $E(\tilde{p}^{LTC})$. This price was published by METI of Japan and equals to 6.8 \$/MMBtu. $\bar{p}^{CPM}$, $\bar{f}^{LTC}$ and $Var(\tilde{p}^{LTC})$ refers to the value we present in Section 5. Through Eq. (B3) and Eq. (B4), we can calculate that γ^s equals to 0.021 and γ^s equals to 0.061. The estimation results show: a) the order of magnitude for risk aversion parameter is around 10^{-2}; b) γ^s is around 3 times of γ^b.

Appendix C: Covariances between LTC and spot LNG prices under different benchmark

$t \in \{1,2,\dots,T\}$	Oil benchmark		JKM benchmark (CIF)		JKM benchmark (FOB)	
$T = 52$	$Cov1$	$Cov2$	$Cov1$	$Cov2$	$Cov1$	$Cov2$
1	-0.0027	0.0065	0.0078	0.0086	0.0079	0.0089
2	-0.0100	-0.0095	0.0215	0.0235	0.0210	0.0231
3	-0.0102	-0.0144	0.0292	0.0324	0.0297	0.0331
4	-0.0062	-0.0108	0.0271	0.0316	0.0277	0.0325
5	-0.0074	-0.0065	0.0207	0.0227	0.0198	0.0221
6	-0.0131	-0.0171	0.0265	0.0256	0.0249	0.0243
7	-0.0115	-0.0153	0.0224	0.0216	0.0207	0.0201
8	-0.0094	-0.0146	0.0221	0.0206	0.0203	0.0190
9	-0.0077	-0.0073	0.0256	0.0234	0.0236	0.0214
10	-0.0168	-0.0161	0.0270	0.0248	0.0254	0.0231
11	-0.0155	-0.0134	0.0313	0.0306	0.0301	0.0292
12	-0.0209	-0.0195	0.0235	0.0234	0.0215	0.0212
13	-0.0293	-0.0256	0.0310	0.0308	0.0287	0.0284
14	-0.0140	-0.0131	0.0267	0.0273	0.0238	0.0243
15	-0.0145	-0.0173	0.0296	0.0299	0.0258	0.0260
16	-0.0182	-0.0194	0.0458	0.0463	0.0419	0.0423
17	-0.0325	-0.0396	0.0413	0.0421	0.0388	0.0393
18	-0.0338	-0.0397	0.0533	0.0532	0.0524	0.0523
19	-0.0537	-0.0551	0.0611	0.0613	0.0602	0.0605
20	-0.0524	-0.0540	0.0720	0.0720	0.0728	0.0726
21	-0.0516	-0.0550	0.0676	0.0674	0.0680	0.0678
22	-0.0517	-0.0557	0.0798	0.0791	0.0796	0.0789
23	-0.0272	-0.0306	0.0812	0.0805	0.0821	0.0814
24	-0.0292	-0.0303	0.0943	0.0942	0.0959	0.0958
25	-0.0230	-0.0222	0.0922	0.0928	0.0935	0.0940
26	-0.0283	-0.0278	0.1053	0.1053	0.1065	0.1065
27	-0.0316	-0.0324	0.1006	0.1006	0.1014	0.1013
28	-0.0217	-0.0205	0.1085	0.1096	0.1093	0.1104
29	-0.0176	-0.0216	0.1277	0.1287	0.1275	0.1285
30	-0.0044	-0.0072	0.1381	0.1391	0.1376	0.1387
31	-0.0062	-0.0039	0.1612	0.1625	0.1618	0.1631
32	-0.0070	-0.0067	0.1669	0.1676	0.1682	0.1691
33	0.0024	0.0027	0.1747	0.1754	0.1748	0.1756

34	-0.0009	-0.0032	0.1935	0.1936	0.1942	0.1943
35	0.0022	0.0018	0.2177	0.2175	0.2191	0.2190
36	0.0096	0.0115	0.2262	0.2262	0.2275	0.2277
37	0.0045	0.0073	0.2426	0.2425	0.2437	0.2436
38	0.0099	0.0138	0.2502	0.2487	0.2523	0.2509
39	0.0133	0.0169	0.2764	0.2747	0.2779	0.2763
40	0.0104	0.0131	0.2998	0.2979	0.3004	0.2987
41	-0.0031	0.0034	0.3310	0.3288	0.3314	0.3295
42	-0.0016	-0.0004	0.3728	0.3710	0.3729	0.3715
43	-0.0006	-0.0008	0.4076	0.4069	0.4078	0.4076
44	0.0103	0.0072	0.4585	0.4582	0.4590	0.4594
45	0.0148	0.0137	0.5101	0.5094	0.5106	0.5108
46	0.0034	-0.0017	0.5564	0.5554	0.5559	0.5561
47	0.0080	0.0049	0.6152	0.6140	0.6141	0.6145
48	-0.0007	-0.0013	0.6842	0.6828	0.6832	0.6841
49	-0.0098	-0.0072	0.7713	0.7695	0.7708	0.7722
50	-0.0093	-0.0122	0.8557	0.8546	0.8559	0.8591
51	-0.0055	-0.0024	0.9490	0.9489	0.9488	0.9546
52	-0.0150	-0.0100	1.0583	1.0586	1.0586	1.0671

Note: $Cov1 = Cov(\tilde{p}^{LTC}, \tilde{p}_t^{SPM})$; $Cov2 = Cov\left(\tilde{p}^{LTC}, \tilde{p}_t^{SPM} - \tilde{f}_t^{SPM}\right)$.